An oncogenic tyrosine kinase inhibits DNA repair and DNA-damage-induced Bcl-x_L deamidation in T cell transformation

Rui Zhao,[1] Feng Tang Yang,[2] and Denis R. Alexander[1]

[1]Laboratory of Lymphocyte Signalling and Development, Molecular Immunology Programme, The Babraham Institute, Babraham, Cambridge CB2 4AT, United Kingdom
[2]Department of Clinical Veterinary Medicine, University of Cambridge, Madingley Road, Cambridge, CB3 0ES, United Kingdom
*Correspondence: denis.alexander@bbsrc.ac.uk

Summary

A transgenic mouse model of T cell lymphoma was used to investigate the transforming events mediated by an oncogenic tyrosine kinase in pretumorigenic $CD4^-CD8^-$ (DN) thymocytes. Parental $CD45^{-/-}$ and $p56^{lck\text{-}F505Y}$ mice do not develop tumors, whereas their $CD45^{-/-}p56^{lck\text{-}F505Y}$ progeny develop T lymphomas. Increased but nononcogenic $p56^{lck}$ kinase activity in $p56^{lck\text{-}F505Y}$ mice DN thymocytes causes cell-cycle progression, survival, and Bcl-X_L upregulation. Additional unique oncogenic signals occur in pretumorigenic $CD45^{-/-}p56^{lck\text{-}F505Y}$ thymocytes in which $p56^{lck}$ kinase activity is 2- to 3-fold higher relative to $p56^{lck\text{-}F505Y}$: inhibition of DNA repair, inhibition of DNA-damage-induced Bcl-X_L deamidation, Bax conformational change and mitochondrial translocation, cytochrome c release, and the apoptotic caspase execution cascade. Inhibition of Bcl-X_L deamidation may be a critical switch in oncogenic kinase-induced T cell transformation.

Introduction

There are more than 90 protein tyrosine kinases in the human genome, of which 30 have been implicated in cancer. The oncogenic tyrosine kinases (OTKs) promote growth factor-independent cell proliferation, protect cells from apoptosis, and render cells resistant to genotoxic therapies (Skorski, 2002). The OTKs employ a wide range of strategies for subverting the normal linkage between DNA damage and cell death. Some OTKs, such as BCR-ABL, inhibit DNA repair (Deutsch et al., 2001), whereas others enhance DNA repair mechanisms in transformed cells, contributing to their genotoxic resistance (Slupianek et al., 2002). In addition, OTKs transmit survival signals that counteract DNA-damage-induced apoptosis (Jain et al., 1996; Skorski, 2002). For example, OTKs have been reported to upregulate the antiapoptotic proteins Bcl-2 and Bcl-X_L (Kumar et al., 1996; Amarante-Mendes et al., 1998), and to inhibit the proapoptotic proteins Bcl-2-associated X protein (BAX) (Wang et al., 1999) and Bcl-2 antagonist of cell death (BAD) (Salomoni et al., 2000). Recently Bcl-X_L deamidation in response to DNA damage has also been described (Deverman et al., 2002), although no link to an OTK has yet been made and the possible role of Bcl-X_L deamidation in oncogenesis remains unknown.

The prevention of DNA-damage-induced apoptosis by the inappropriate upregulation of survival pathways is one of the hallmarks of cellular transformation (Hanahan and Weinberg, 2000). The actions of OTKs in regulating these processes have been investigated mainly using transformed cells, whereas less information is available concerning the role of OTKs in early oncogenic events in primary cells. The murine thymus provides a useful experimental system for the investigation of such events. The $CD4^-CD8^-$ (double negative, DN) thymic population, comprising 1%–3% of the adult thymus, can be subdivided into four discrete developmental stages: the $CD25^-CD44^+$ (DN1), $CD25^+CD44^+$ (DN2), $CD25^+CD44^-$ (DN3), and $CD25^-CD44^-$ (DN4) subsets (Rodewald and Fehling, 1998). Successful TCRβ rearrangements lead to expression of the pre-TCR on DN3 thymocytes and the subsequent $p56^{lck}$ tyrosine kinase-dependent mediation of survival and proliferative signals in a process known as β selection.

We have recently generated a mouse cancer model in which aggressive T lineage thymic tumors develop in 100% of $CD45^{-/-}$ animals expressing mutant $p56^{lck\text{-}F505}$ in which the inhibitory regulatory Tyr-505 at the C terminus has been mutated to a Phe (Baker et al., 2000). CD45 is a transmembrane tyrosine phosphatase that is expressed abundantly on hematopoietic cells (Alexander, 1997), and $CD45^{-/-}$ mice are characterized by defects in thymic development but no tumorigenesis (Byth et al., 1996). In the parental low copy number *lck*^{F505} (PLGF-A) mice bred with $CD45^{-/-}$ mice, the mutant *lck* transgene causes premature

SIGNIFICANCE

We have shown that an oncogenic tyrosine kinase inhibits DNA repair in pretumorigenic primary murine thymocytes, resulting in genomic instability and chromosomal aberrations. Elimination of the DNA-damaged cells is blocked by a powerful prosurvival pathway that inhibits the mitochondrial-regulated cascade of events that lead to apoptosis. This pathway prevents the Bcl-X_L deamidation that normally occurs following DNA damage and preserves the ability of Bcl-X_L to sequester a proapoptotic BH3-only-containing protein such as Bim. The oncogenic kinase therefore appears to transform T cells by a "double whammy" whereby DNA damage is promoted but Bcl-X_L prosurvival functionality is simultaneously maintained, thereby disrupting the cancer protection pathway that normally disposes of cells with damaged DNA.

allelic exclusion, but no tumors; much higher expression of the active *lck*^{F505} transgene can generate thymic tumors in the CD45$^{+/+}$ thymus (Abraham et al., 1991). On a CD45$^{-/-}$ background, the positive regulatory Tyr-394 site in p56^{lck} becomes hyperphosphorylated in the low copy number *lck*^{F505} (PLGF-A) murine thymocytes, presumably because CD45 is not available to dephosphorylate this residue, thereby switching the p56^{lck} kinase to a hyperactive oncogenic state (Baker et al., 2000). The CD45$^{-/-}$Lck^{F505} tumor cells are phenotypically characteristic of the DN3/DN4 stage of thymic differentiation. Tumor incidence is the same in CD45$^{-/-}$Lck^{F505} mice backcrossed to the Rag-1$^{-/-}$ background (Baker et al., 2000).

In the present work we have analyzed the signaling pathways in pretumorigenic DN CD45$^{-/-}$Lck^{F505} thymocytes that lead to transformation in relation to p56^{lck} kinase activity and function. Whereas the nononcogenic "intermediate level" mutant p56$^{lck\text{-}F505}$ activity (Alexander, 2000) induces a powerful survival signal in Rag$^{-/-}$CD45$^{-/-}$ thymocytes, involving Bcl-X_L upregulation and causing rescue of the DN3 and DN4 subsets from apoptosis, the oncogenic hyperactive mutant p56$^{lck\text{-}F505}$ activity that characterizes CD45$^{-/-}$Lck^{F505} thymocytes triggers two additional critical signals: inhibition of DNA damage repair, leading to marked genomic instability, and stimulation of a distinct survival pathway that prevents DNA-damage-induced apoptosis.

Results

p56^{lck} is hyperactive in DN CD45$^{-/-}$Lck^{F505} thymocytes

Four different mouse lines were used to carry out this study: wild-type C57BL/6, Lck^{F505} (PLGF-A), CD45$^{-/-}$, and the CD45$^{-/-}$Lck^{F505} progeny of Lck^{F505} × CD45$^{-/-}$ crosses. Only the CD45$^{-/-}$Lck^{F505} progeny developed thymic tumors. All experiments described were carried out on pretumorigenic thymocytes from 5- to 8-week-old mice. In addition, we utilized for technical reasons the same lines backcrossed to a Rag-1$^{-/-}$ background. Flow cytometric analyses of the mice used for this study can be found in the Supplemental Data (Supplemental Figure S1 at http://www.cancercell.org/cgi/content/full/5/1/37/DC1). Figure 1A (middle panel) shows that the expression of p56^{lck} in DN thymocyte lysates from the lines expressing the mutant Lck^{F505} transgene was 2.3 ± 0.2 (n = 4) fold higher than wild-type or CD45$^{-/-}$ DN thymocytes. We have previously shown that the p56^{lck} kinase activity in CD45$^{-/-}$Lck^{F505} thymocytes is increased about 2-fold in relation to wild-type thymocytes, correlating with increased phosphorylation at the positive regulatory site Tyr-394 (Baker et al., 2000). A more detailed analysis of these parameters was necessary for two reasons: first, our earlier biochemical studies were carried out using whole thymocytes, whereas transformation occurs at the DN differentiation stage (Baker et al., 2000) and the regulation of p56^{lck} could differ between the dominant DP and minor DN subsets; second, the commercial antibody that we used in our previous study to measure p56^{lck} Tyr-394 phosphorylation (Baker et al., 2000) was, in the interim, withdrawn. We have therefore obtained a new and well-characterized pTyr-394 antibody (Holdorf et al., 2002) for use in the present work.

To facilitate the analysis of p56^{lck} in DN subsets, we utilized mice on the Rag-1$^{-/-}$ background, since virtually all thymocytes in Rag-1$^{-/-}$ and Rag-1$^{-/-}$CD45$^{-/-}$ mice are CD4$^-$CD8$^-$. In addition, highly purified DN subsets were prepared from Rag-1$^{-/-}$Lck^{F505} and Rag-1$^{-/-}$ CD45$^{-/-}$Lck^{F505} mice in which the active *lck* transgene promotes the DN to DP transition (Pingel et al., 1999). Figure 1A (upper panel) shows that pTyr-505 was hyperphosphorylated in CD45$^{-/-}$Rag-1$^{-/-}$ compared to Rag-1$^{-/-}$ DN thymocytes, consistent with our previous results using whole thymocytes (Stone et al., 1997). As expected, pTyr-505 phosphorylation was not prominent in cells expressing the mutant lck^{F505} transgene. There was a marked 4-fold increase in pTyr-394 phosphorylation in Rag-1$^{-/-}$CD45$^{-/-}$Lck^{F505} compared to Rag-1$^{-/-}$Lck^{F505} thymocytes. In vitro kinase assays revealed that the p56^{lck} kinase activity was more than 5-fold higher in Rag-1$^{-/-}$CD45$^{-/-}$Lck^{F505} compared to Rag-1$^{-/-}$ DN thymocytes, and more than 2-fold higher when compared with Rag-1$^{-/-}$CD45$^{-/-}$ or Rag-1$^{-/-}$Lck^{F505} mice (Figure 1B). Interestingly, a prominent 34–36 kDa phosphorylated protein (as yet unidentified) was found in association with the high activity p56^{lck}. Overall, these results are consistent with the model that CD45 can dephosphorylate both pTyr-394 and pTyr-505 p56^{lck} regulatory sites in DN thymocytes. Furthermore, p56^{lck} kinase activities in DN thymocytes may be defined as basal (Rag-1$^{-/-}$), intermediate (Rag-1$^{-/-}$CD45$^{-/-}$ or Rag-1$^{-/-}$Lck^{F505}), or hyperactive (Rag-1$^{-/-}$CD45$^{-/-}$Lck^{F505}) (Alexander, 2000). Further studies were directed toward answering the key question: what are the signaling switches triggered by oncogenic hyperactive p56^{lck} that are distinct from those induced by nononcogenic intermediate activity p56^{lck}?

Intermediate activity and hyperactive p56^{lck} are equally proficient in promoting the survival and cell cycle progression of DN thymocytes

We considered that hyperactive p56^{lck} might trigger oncogenic events by causing abnormally high survival of DN3 thymocytes that fail β selection and/or by perturbing the cell cycle. This question is most readily addressed using Rag-1$^{-/-}$ thymocytes in which the complete failure of β selection leads to a high level of thymic apoptosis (Falk et al., 2001). Figure 2 shows that in the Rag-1$^{-/-}$ DN3 subset, 90% or more of cells are apoptotic. However, even the 2-fold higher p56^{lck} activity found in Rag-1$^{-/-}$CD45$^{-/-}$ thymocytes is sufficient to rescue about 70% of the cells, and essentially, complete rescue was induced by the mutant kinase transgene in both Rag-1$^{-/-}$Lck^{F505} and Rag-1$^{-/-}$CD45$^{-/-}$Lck^{F505} thymocytes. The greater prosurvival potency of "intermediate activity" mutant p56$^{lck\text{-}F505}$, when compared to wild-type p56^{lck} on a CD45$^{-/-}$ background, is most likely explained by the greater accessibility of the noncatalytic domains in the mutant Y505F form of the kinase (Stone et al., 1997; Lin et al., 2000).

We next investigated the cell cycle by assessing 7-AAD staining in DN subsets. As expected, nearly all Rag-1$^{-/-}$ and Rag-1$^{-/-}$CD45$^{-/-}$ DN3 cells were in growth arrest due to their lack of pre-TCR mediated mitogenic signals, whereas Lck^{F505}, as previously described (Pingel et al., 1999), promoted cell-cycle progression (Figure 3A). Significantly, however, the percentages of DN3 and DN4 Rag-1$^{-/-}$CD45$^{-/-}$Lck^{F505} thymocytes in cycle were no greater or less despite their hyperactive p56^{lck}. Furthermore, detailed analysis of the percentages of DN3 and DN4 cells in the S, G2, and M phases of the cell cycle revealed no significant differences between the Rag-1$^{-/-}$Lck^{F505} and Rag-1$^{-/-}$CD45$^{-/-}$Lck^{F505} thymus (data not shown). We considered that in vivo BrdU incorporation might provide a more dynamic insight into the turnover of thymic subsets. Figure 3B shows that whereas DNA synthesis was markedly suppressed in Rag-

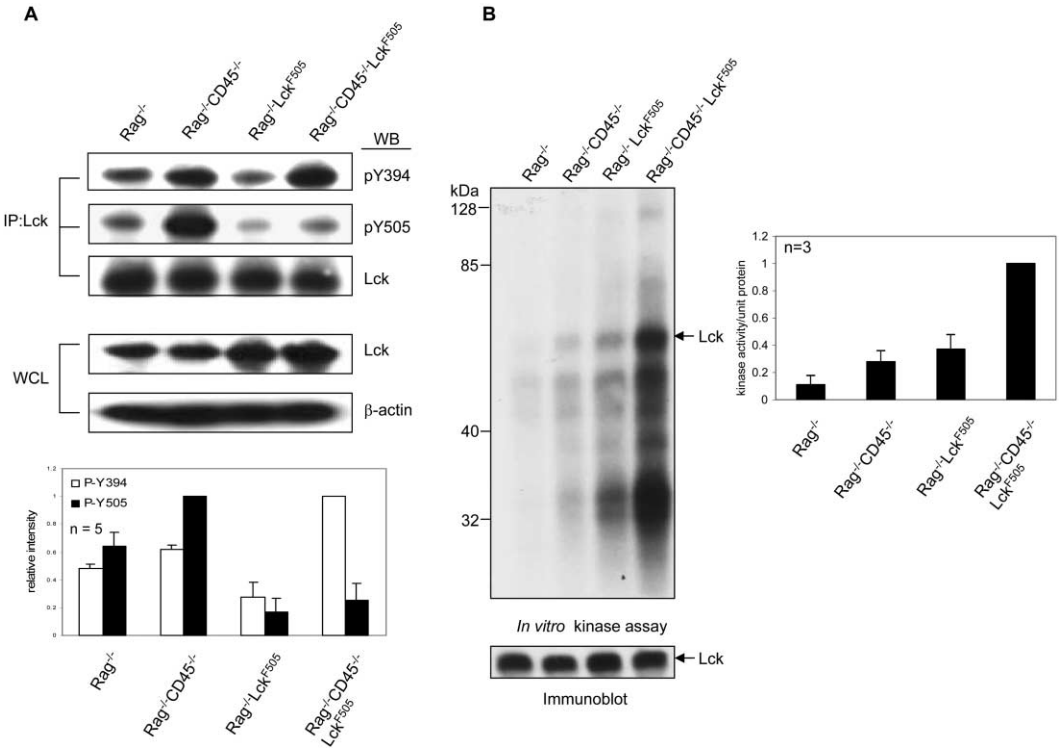

Figure 1. p56^{lck} pTyr-394 phosphorylation and kinase activity are upregulated in Rag$^{-/-}$CD45$^{-/-}$Lck^{F505} DN thymocytes

A: Immunoprecipitated p56^{lck} from DN thymocytes was blotted for p-Tyr394, followed by stripping and reprobing for p-Tyr505, and then for p56^{lck} protein to demonstrate comparable loading (upper panel). The histogram data represent means ±SD from five independent experiments and are expressed as relative phosphorimager values normalized for p56^{lck} loading. Whole cell lysates were immunoblotted for p56^{lck} and phosphorimager values (see text) normalized using actin as a loading control (middle panel).

B: In vitro kinase assays of p56^{lck} immunoprecipitated from DN thymocytes immunoblotted for p56^{lck} to show comparable loading. The histogram shows mean p56^{lck} relative autophosphorylation values from three independent experiments normalized for p56^{lck} loading.

1$^{-/-}$ and Rag-1$^{-/-}$CD45$^{-/-}$ DN3 cells and, as expected, promoted by Lck^{F505}, no greater increase in DNA synthesis was observed in DN3 and DN4 pretumorigenic Rag-1$^{-/-}$CD45$^{-/-}$Lck^{F505} as compared to Rag-1$^{-/-}$Lck^{F505} thymocytes.

Overall, these results show that DN3/DN4 thymocyte survival and cell cycle progression are exquisitely sensitive to the p56^{lck} activity level, but the data do not discriminate between the oncogenic and nononcogenic consequences of p56^{lck} signaling.

Hyperactive p56$^{lck\text{-}F505}$ inhibits DNA repair and promotes genomic instability

We used pulsed field gel electrophoresis (PFGE) to assess the efficiency of DNA repair mechanisms (De Silva et al., 2000). Purified DN thymocytes were exposed to ionizing irradiation, then fixed immediately or left for 6 hr or 24 hr for DNA repair to occur before assessing the level of DNA damage. Figure 4Aa shows that the rapid increase in DSBs following irradiation, as revealed by the decrease in average fragment length, was comparable in the four mouse lines under investigation. Interestingly, however, whereas DSB repair was essentially complete after 24 hr in the thymocytes with basal and intermediate p56^{lck} activities, in DN CD45$^{-/-}$Lck^{F505} thymocytes, repair was markedly inhibited. The repair efficiency in the thymocytes expressing oncogenic Lck^{F505} was reduced by about 4-fold at 24 hr in comparison with CD45$^{-/-}$ and Lck^{F505} thymocytes (viz. about 70% of DNA still contained DSBs compared to 15%–20% in the control cells). The increase in DNA molecular weight to >5.7 Mb from 1.7–3.0 Mb in control cells at 6 hr (lanes 11–13) confirms that repair was occurring, and this partial repair was also much reduced in pretumorigenic thymocytes (lane 14). The rapidity of fragmentation after irradiation and the pattern of repair confirm that these results represent DNA damage and repair, and not apoptosis (Cohen et al., 1994). Overall, the data show that one or more DNA repair mechanisms is strongly inhibited only in the cells expressing oncogenic hyperactive p56$^{lck\text{-}F505}$.

It is thought that of all forms of DNA damage, DSBs are particularly potent in generating genomic instability (Khanna and Jackson, 2001), resulting in chromosomal translocations with oncogenic potential (Richardson and Jasin, 2000). We therefore carried out two separate types of assay to assess genomic instability in the primary pretumorigenic CD45$^{-/-}$Lck^{F505} DN thymocytes. The first depends on the finding that DSBs induce histone H2AX phosphorylation on Ser-139 (Rogakou et al., 1998). Recently, H2AX has been shown to be an important suppressor of oncogenic translocations and tumors (Bassing et al., 2003). Figure 4Ab shows that a phosphospecific antibody against γ-H2AX, the phosphorylated form of the protein, revealed a strong signal by immunoblotting in purified CD45$^{-/-}$Lck^{F505} DN thymocytes, but not in control cells. The flow cytometric

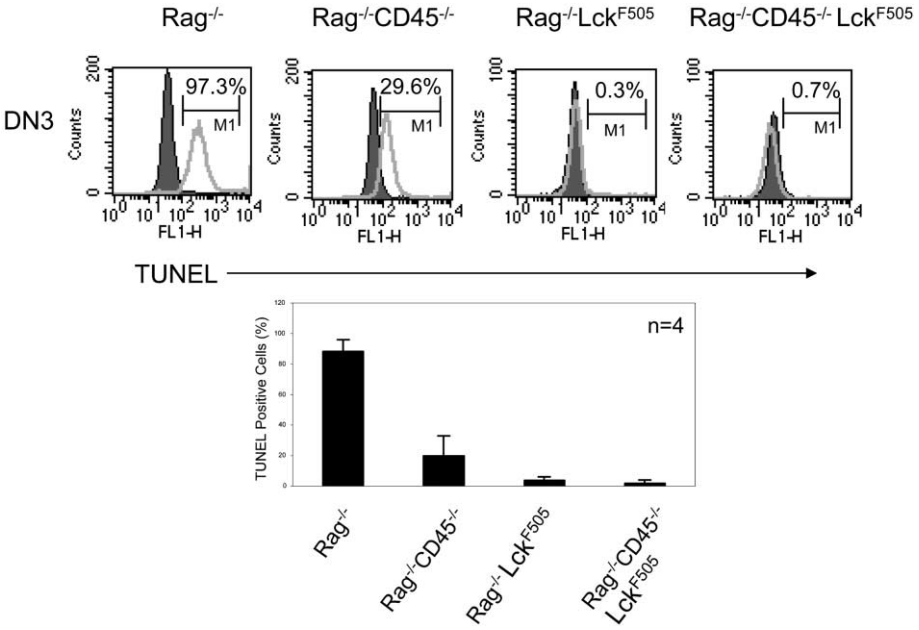

Figure 2. The survival of DN3 thymocytes is promoted to a comparable extent by nononcogenic or oncogenic p56$^{lck\text{-}F505}$

TUNEL assays were used to assess apoptosis in gated DN3 cells represented by the gray line; controls were carried out by adding all reagents except for Tdt (dark area). The histogram is based on four independent experiments and shows mean TUNEL positive cells ±SD.

data illustrated in Figure 4Ac also show that the staining for γ-H2AX is about 5-fold higher in Rag$^{-/-}$CD45$^{-/-}$Lck^{F505} DN3/4 thymocytes as compared to controls. Taken together, these results demonstrate a higher level of γ-H2AX in primary pretumorigenic DN thymocytes, consistent with an increased load of DSBs. Since each DSB is thought to cause the phosphorylation of multiple H2AX molecules, this most probably explains why this more sensitive assay reveals increased DSBs under

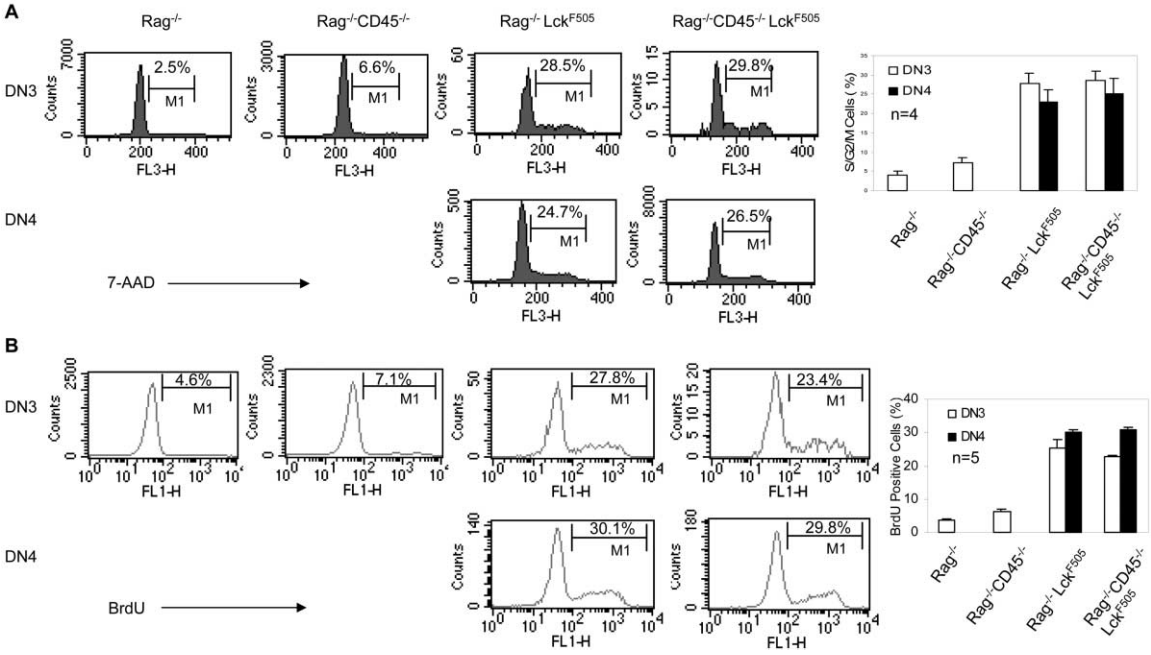

Figure 3. Nononcogenic or oncogenic Lck^{F505} drives Rag$^{-/-}$ and Rag$^{-/-}$CD45$^{-/-}$ DN3 and DN4 thymocytes into cell cycle to a comparable extent

A: Cell cycle analysis of DN3 and DN4 thymocytes based on 7-AAD staining. Percentages of the cells in the S/G2/M phases in the DN3 and DN4 subsets are shown in each frame. The histogram is based on four independent experiments and shows means ±SD.

B: BrdU in vivo labeling. BrdU staining was measured in DN3 and DN4 subsets 2 hr postinjection. The histogram is based on five independent experiments and shows means ±SD. Note that DN4 subsets are not shown for Rag$^{-/-}$ and CD45$^{-/-}$Rag$^{-/-}$ subsets because development is blocked at the DN3 stage. This also explains why the cell counts analyzed on the *y* axes are high for Rag$^{-/-}$ and CD45$^{-/-}$Rag$^{-/-}$ DN3 subsets, but low when Lck^{F505} is present, because it causes progression to the DP maturation stage, so "emptying" the DN3 compartment (Supplemental Figure S1 at http://www.cancercell.org/cgi/content/full/5/1/37/DC1).

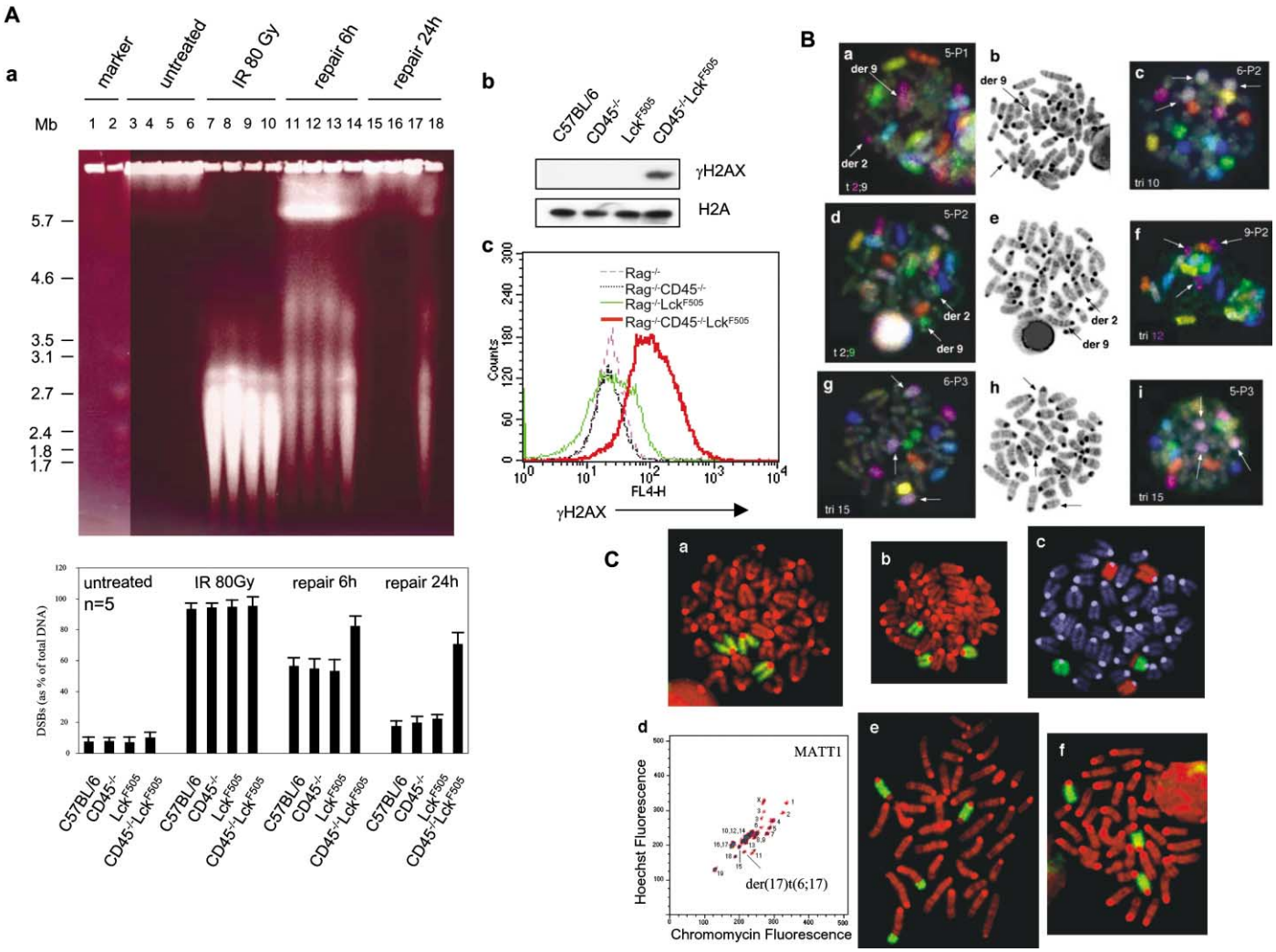

Figure 4. Oncogenic Lck^{F505} inhibits DNA repair and promotes chromosomal instability

A: Analysis of DNA damage and repair in purified DN thymocytes. **a:** Pulse field gel electrophoresis analysis of DNA from γ irradiated purified DN thymocytes. Thymocytes from C57BL/6 (lanes 3, 7, 11, and 15), CD45$^{-/-}$ (lanes 4, 8, 12, and 16), Lck^{F505} (lanes 5, 9, 13, and 17) and CD45$^{-/-}$Lck^{F505} (lanes 6, 10, 14, and 18) mice were treated as indicated. The S. pombe (lane 1) and H. wingei (lane 2) chromosomes were used as DNA size markers (note that the markers were clearer in the original gel than illustrated here). The results, based on 5 separate experiments, have been quantified by scanning the gel with a phosphorimager and estimating the relative DSBs as the DNA remaining in the gel as a % of total DNA in each lane. **b:** DN thymocytes purified from C57BL/6, CD45$^{-/-}$, Lck^{F505}, and CD45$^{-/-}$Lck^{F505} mice were immunoblotted for γH2AX. The membrane was stripped and reprobed for H2A. **c:** Expression of γH2AX analyzed by flow cytometry. Permeabilized thymocytes staining positive for FITC-conjugated CD3, CD4, CD8, and CD44 mAbs were gated out and a biotinylated γH2AX mAb was used to stain the DN3/DN4 thymic subsets.

B: Chromosomal aberrations (arrowed) in purified DN thymocytes revealed by rainbow FISH probes. **a:** P1 onto Mouse 5 (Rag$^{-/-}$CD45$^{-/-}$Lck^{F505}) showing a t2;9 translocation. The derived chromosomes (colored mauve) are indicated as "der 2" and "der 9": "der 2" is the derived chromosome that carries the centromeric portion of chromosome 2. Note that chromosome 9 is invisible in this pool (see **d** for chromosome 9). **b:** DAPI-banded metaphase shown in **a**. **c:** P2 onto Mouse 6 (Rag$^{-/-}$CD45$^{-/-}$Lck^{F505}) showing the trisomy 10. **d:** P2 onto Mouse 5 showing the t2;9 translocation. Note that only the green chromosome 9 portion of the translocation is present in this pool. The derived chromosomes are indicated as "der 2" and "der 9." **e:** DAPI-banded metaphase shown in **d**. **f:** P2 onto Mouse 9 (CD45$^{-/-}$Lck^{F505}) showing a partial trisomy 12. **g:** P3 onto Mouse 6 (male) showing a trisomy 15. **h:** DAPI-banded metaphase shown in **g**. **i:** P3 onto Mouse 5 (female) showing a trisomy 15.

C: Characterization of the karyotypes of MATT-1 and MATT-4 cell lines. **a:** Hybridization of mouse chromosome 4 paint (green) onto MATT-1 chromosomes (red). **b:** Hybridization of mouse chromosome 14 paint (green) onto MATT-1 chromosomes (red). **c:** Simultaneous hybridization of mouse chromosome paints 6 (red) and 17 (green) onto MATT-1 chromosomes (blue). **d:** A bivariate flow karyotype of the MATT-1 cell line. **e:** Hybridization of paint from the der (17)t(6;17) onto the C3H metaphase (red). **f:** Hybridization of mouse chromosome 15 paint (green) onto MATT-4 metaphase (red).

basal conditions, whereas PFGE does not (cf. Figure 4Aa lanes 3–6).

In the second type of assay to assess genomic instability we carried out karyotype analysis by chromosome painting (Ferguson-Smith, 1997) on purified DN thymocytes cultured in IL-4 to obtain metaphase spreads (Zlotnik et al., 1987). Flow cytometric analysis confirmed that DN thymic subsets did not detectably change their surface marker phenotypes with reference to CD3, CD4, CD8, CD25, and CD44 under the culture conditions used (data not shown). No chromosomal abnormali-

ties were detected in 43 metaphase spreads from either CD45$^{-/-}$ or Lck^{F505} control DN thymocytes (data not shown). However, as Figure 4B illustrates, multiple chromosomal abnormalities were detected in pretumorigenic DN thymocytes from three out of five CD45$^{-/-}$Lck^{F505} mice analyzed. Thus, Mouse 5 displayed a t2;9 translocation (Figures 4Ba and 4Bd) and a trisomy 15 (i), Mouse 6 a trisomy 10 (c) and a trisomy 15 (g), and Mouse 9 a partial trisomy 12 (f). These results confirm marked genomic instability uniquely in pretumorigenic DN CD45$^{-/-}$Lck^{F505} thymocytes. To establish whether chromosomal abnormalities in tumor cells might be similar to those in the pretumorigenic thymocytes, we established cell lines from the tumors of individual CD45$^{-/-}$Lck^{F505} mice (MATT-1 and MATT-4) and carried out chromosomal analysis on early passage cells. Hybridizations revealed multiple chromosomal abnormalities involving trisomies of chromosomes 4, 6, and 14, an apparently unbalanced 6:17 translocation in MATT-1 cells (Figures 4Ca–4Ce), and a trisomy 15 in MATT-4 cells (Figure 4Cf). To determine the origin of the 6:17 translocation in MATT-1 cells, the derivative chromosome was sorted by flow cytometry (Figure 4Cd) and made into a paint, which was hybridized onto normal metaphases from a C3H mouse (Figure 4Ce). Chromosome painting revealed that the der(17)t(6:17) is composed of two chromosomal segments: one segment from 6qF1-G3 and the other from 17qA1-E1, and that 17qE2-E5 has been deleted during translocation (Figure 4Ce). Therefore, tumors from CD45$^{-/-}$Lck^{F505} mice also display evidence of chromosomal damage, including nonreciprocal translocations, which are common in human cancer but rare in mice.

Overall, these findings demonstrate a striking correlation between inhibition of DNA repair and genomic instability in primary pretumorigenic DN thymocytes expressing oncogenic p56$^{lck\text{-}F505}$, although this did not result in consistent patterns of chromosomal abnormality in either pretumorigenic or tumor CD45$^{-/-}$Lck^{F505} cells.

A powerful survival pathway prevents DNA-damage-induced apoptosis in thymocytes expressing hyperactive p56$^{lck\text{-}F505}$

We surmised that since DNA repair is inhibited and DNA damage increases in primary DN thymocytes (Figure 4), the DNA damage response that normally leads to apoptosis might be disrupted in CD45$^{-/-}$Lck^{F505} thymocytes. To investigate this possibility, we exposed thymocytes to ionizing irradiation or to etoposide and then investigated the sub-G1 peak of 7-AAD stained DN3 and DN4 cells to assess the extent of apoptosis (Figure 5A). The marked increase in apoptosis that occurred in response to DNA damage was comparable in C57BL/6, Lck^{F505} and CD45$^{-/-}$ thymocytes, whereas in both the DN3 and DN4 Lck^{F505}CD45$^{-/-}$ subsets, the sub-G1 peaks were close to untreated levels, indicating that only in the thymocytes expressing oncogenic p56$^{lck\text{-}F505}$ was there a powerful survival signal protecting the cells from apoptosis. This is in sharp contrast to the comparable efficiency of either intermediate or hyperactive p56^{lck} in rescuing DN thymocytes from apoptosis following the failure of β selection (Figure 2).

A hallmark of DNA damage in normal cells is the induction, phosphorylation, and consequent activation of the p53 transcription factor resulting in cell cycle arrest and apoptosis (Sherr and McCormick, 2002; Vousden and Lu, 2002). Since the functional loss of p53 is a common characteristic of tumor cells, thereby effecting escape from apoptotic surveillance (Bullock and Fersht, 2001), we examined the ability of DNA damage to regulate p53 and its downstream effectors. Figure 5B shows that DNA-damage-induced p53 protein and pSer-15 phoshorylation (Siliciano et al., 1997) levels were, if anything, higher in the pretumorigenic Lck^{F505}CD45$^{-/-}$ thymocytes than in the parental or wild-type controls. Furthermore, the downstream p53 effectors Mdm2, Bax, and p21^{WAF1} were likewise induced at somewhat higher levels in the thymocytes expressing hyperactive p56$^{lck\text{-}F505}$ (Figure 5C). Interestingly, purified pretumorigenic DN Rag$^{-/-}$Lck^{F505}CD45$^{-/-}$ thymocytes displayed increased p53 activation even without prior DNA-damaging treatments, whereas p53 was hyperactivated in Lck^{F505}CD45$^{-/-}$ tumor cells (Figure 5D). Overall, these results demonstrate that the linkage between DNA damage and p53 regulation is intact in Lck^{F505}CD45$^{-/-}$ thymocytes.

Oncogenic p56$^{lck\text{-}F505}$ selectively inhibits Bcl-X$_L$ deamidation, Bax translocation, and the caspase cascade

Since p53 was clearly functional, we investigated the downstream caspase execution apparatus of the apoptotic pathway (Hengartner, 2000) and then worked back upstream to identify the locus of action of oncogenic p56$^{lck\text{-}F505}$. In mammals, cytochrome c initiates caspase activation following its release from mitochondria and subsequent oligomerization with multimeric Apaf-1 to form the active apoptosome complex (Zou et al., 1999; Wang, 2001a). This in turn activates procaspase-9, which activates executioner caspases such as caspase-3 (Rodriguez and Lazebnik, 1999), which in turn can cleave the 113 kDa form of poly(ADP-ribose)polymerase (PARP) to yield an inactive 89 kDa fragment (Simbulan-Rosenthal et al., 1999). Figure 6A shows that whereas DNA damage induced effective PARP cleavage in thymocytes expressing basal or intermediate p56^{lck} activities, cleavage was almost completely inhibited in Lck^{F505}CD45$^{-/-}$ thymocytes. Inhibition of caspase-3 activation following DNA damage was confirmed by the demonstration that the conversion of 32 kDa procaspase-3 to active 17 kDa caspase-3 was blocked only in thymocytes expressing hyperactive p56$^{lck\text{-}F505}$ (Figure 6B).

Since our results suggested that caspase-9 activation was inhibited, we next measured mitochondrial cytochrome c release before and after cell exposure to etoposide. As Figure 6C illustrates, DNA damage triggered a marked release of cytochrome c into the cytosol in C57BL/6, Lck^{F505}, and CD45$^{-/-}$ thymocytes, but release was barely detectable in Lck^{F505} CD45$^{-/-}$ thymocytes. It has previously been shown that translocation of the proapoptotic molecule Bax to the mitochondria is critical in cytochrome c release (Gross et al., 1998). By stripping and reprobing the membrane with Bax antibody, we showed that Bax translocation to mitochondria was prevented only in Lck^{F505}CD45$^{-/-}$ thymocytes, correlating precisely with the block in cytochrome c release (Figure 6C). Mitochondrial and cytosolic fraction integrity and equal loading were confirmed by further probing the Western blot with antibodies for cytochrome oxidase subunit IV (Cox-IV) and tubulin, respectively. A conformational change in Bax precedes its translocation to mitochondria, and the 6A7 mAb recognizes an epitope in its N terminus that becomes exposed during apoptotic signaling (Hsu and Youle, 1998; Nechushtan et al., 1999). We therefore immunoprecipitated Bax with 6A7 mAb from thymic lysates before and after etoposide treatment, using Chaps detergent to preserve the integrity of the epitope,

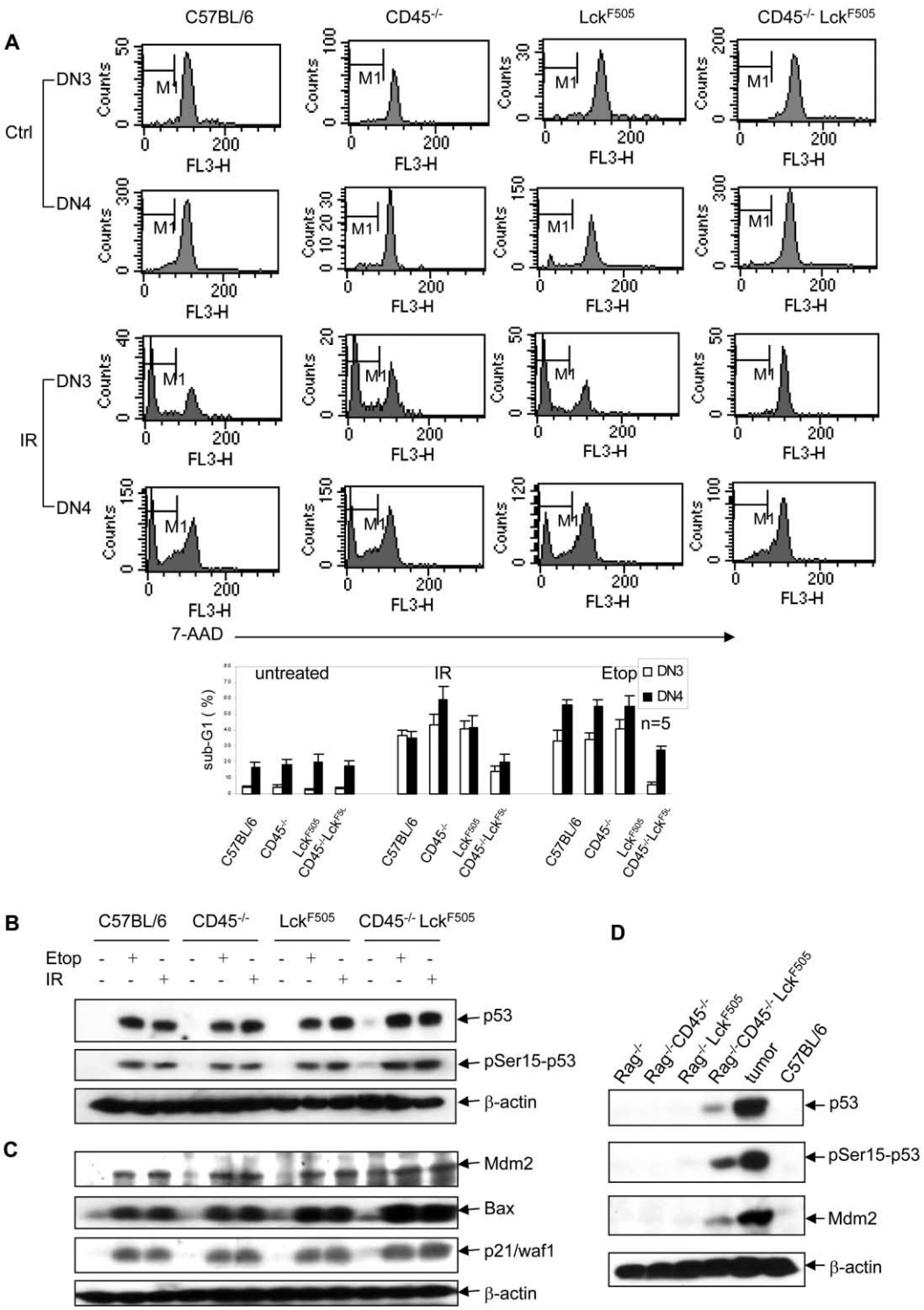

Figure 5. Oncogenic Lck^{F505} inhibits DNA-damage-induced apoptosis but not p53 induction

A: Thymocytes were nonexposed (Ctrl) or exposed to 10 Gy γ irradiation (IR), then cultured in appropriate media or in the presence of 50 μM etoposide (Etop), before staining with 7-AAD, and subjected to FACS analysis 24 hr later. A representative experiment is shown and the histogram illustrates the means from five independent experiments ±SD, including both the IR and Etop data.

B: Thymocytes were exposed to DNA-damaging conditions as in **A** followed by immunoblotting for p53 or pSer-15-p53. The membrane was stripped and reprobed for actin to confirm comparable loading.

C: Immunoblotting for Mdm2, Bax, and p21^{WAF-1} on the same membrane, with actin for loading, using the same experimental conditions as in **B**.

D: DN thymocytes purified from Rag$^{-/-}$Lck^{F505} and Rag$^{-/-}$CD45$^{-/-}$Lck^{F505} mice (5 of each), or thymocytes from Rag$^{-/-}$, Rag$^{-/-}$CD45$^{-/-}$, and C57BL/6 mice, or Rag$^{-/-}$CD45$^{-/-}$Lck^{F505} tumor cells, were immunoblotted for p53, pser15-p53, and Mdm2 (10^7 cells per track).

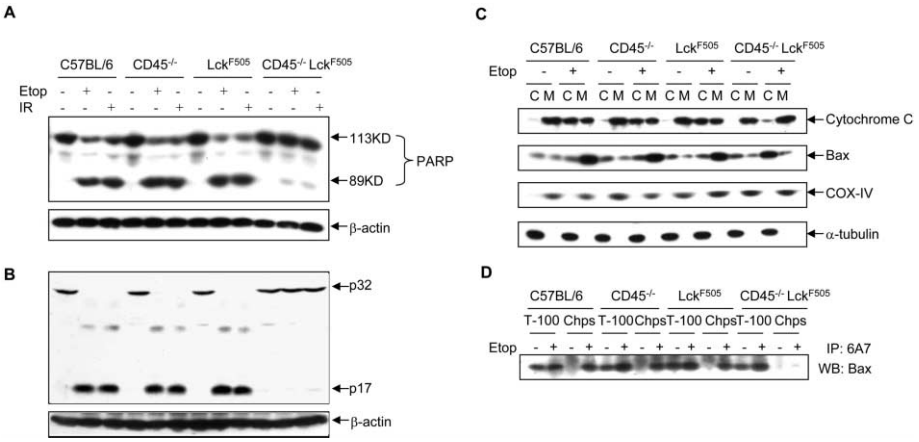

Figure 6. Oncogenic Lck^{F505} inhibits DNA-damage-induced Bax conformational change, Bax translocation, cytochrome c release, and the caspase activation cascade

Cells were treated exactly as in Figure 5 and immunoblotted as shown.

A: Immunoblotting was performed using a mAb that recognizes the full length and cleaved forms of PARP.

B: A caspase-3 ab was used that detects both the pro- (p32) and activated (p17) forms of caspase-3.

C: Cytosolic and mitochondrial fractions were immunoblotted for cytochrome c and Bax. The membrane was stripped and reprobed for cytochrome oxidase subunit IV (COX-IV) and α-tubulin as markers for mitochondria and cytosol, respectively.

D: Cells were cultured with or without etoposide for 24 hr, then lysed with buffer containing either 1% Triton X-100 (T100) or 1% Chaps (Chps). The change in Bax conformation was measured by immunoprecipitating Bax with the 6A7 mAb followed by immunoblotting with a polyclonal Bax ab.

followed by immunoblotting for Bax. Parallel immunoprecipitations were carried out using Triton X-100 lysates as a positive control, as this detergent changes Bax conformation to expose the 6A7 epitope (Hsu and Youle, 1998). Figure 6D shows that DNA damage caused a striking change in Bax conformation in thymocytes expressing basal or intermediate activity $p56^{lck}$, whereas this conformational change was blocked in the presence of hyperactive $p56^{lck}$. These results suggest that the survival pathway mediated by oncogenic $p56^{lck\text{-}F505}$ lies upstream of Bax conformational change.

Proapoptotic Bcl-2 members can be divided into the "multidomain" family members, which possess homology in BH1-3 domains, such as Bax, and the "BH3 domain only" members, which display sequence homology only within this critical death domain (Huang and Strasser, 2000). It is thought that the BH1-3 proteins may be the primary effectors of apoptosis, whereas the BH3-only proteins regulate Bax or Bak functions. For example, the BH3-only proteins Bid or Bim bind to Bax to promote the release of mitochondrial proteins, and antiapoptotic molecules such as Bcl-2 or Bcl-X_L can act by binding and sequestering Bid or Bim, thereby preventing their proapoptotic interactions with Bax (Cheng et al., 2001; Kuwana et al., 2002). We first showed (by FACS analysis) that Bcl-2 expression levels are comparable between the DN1-DN4 thymic subsets in the four mouse lines under investigation (data not shown). By contrast, immunoblotting revealed that Bcl-X_L expression was increased in both Rag-$1^{-/-}Lck^{F505}$ and Rag-$1^{-/-}CD45^{-/-}Lck^{F505}$ purified DN thymocytes relative to controls, and tumor cell expression was even higher (Figure 7A, upper panel). FACS analysis of specific DN $Rag^{+/+}$ thymic subsets stained for Bcl-X_L showed that whereas expression in DN3 cells was comparable in the four lines under investigation, distinct Bcl-X_L^- and Bcl-X_L^+ populations of $CD45^{-/-}$ DN4 cells were detectable (data not shown). However, in both the Lck^{F505} and $CD45^{-/-}Lck^{F505}$ thymus, the DN4 cells were nearly all Bcl-X_L^+, consistent with the results shown in Figure 7A. Since the increase in Bcl-X_L expression was comparable in the "intermediate" and "hyperactive" $p56^{lck}$ kinase activity cells, this observation alone does not explain why only the $Rag^{-/-}CD45^{-/-}Lck^{F505}$ thymocytes develop tumors.

Interestingly, Bcl-X_L deamidation in response to DNA damage has been proposed as a critical switch to subvert the prosurvival function of Bcl-X_L (Deverman et al., 2002). Figure 7A (lower panel) shows that in untreated thymocytes, Bcl-X_L migrates as a doublet, and that the faster migrating species effectively disappears following DNA damage. This is consistent with the previous work based on an osteosarcoma cell line demonstrating that this shift is caused by the deamidation of two asparagine residues (Asn 52 and Asn 66) (Deverman et al., 2002; Aritomi et al., 1997). Remarkably, this characteristic shift did not occur in $Lck^{F505}CD45^{-/-}$ thymocytes following exposure to either etoposide or γ irradiation (Figure 7A), suggesting that oncogenic $p56^{lck\text{-}F505}$ inhibits deamidation. Since the antiapoptotic function of Bcl-X_L mirrors its ability to sequester BH3-only proteins (Cheng et al., 2001), we investigated Bcl-X_L binding to Bim as an exemplar of this interaction. Figure 7B shows that after etoposide treatment, the Bcl-X_L level found in Bim immunoprecipitates was much higher in hyperactive $p56^{lck\text{-}F505}$ thymocytes than in cells expressing basal or intermediate $p56^{lck}$ activity levels. Likewise, the Bim signal was elevated uniquely in Bcl-X_L immunoprecipitates from $Lck^{F505}CD45^{-/-}$ thymocytes (Figure 7B). Three splice forms of Bim have been described: Bim_S, Bim_L, and Bim_{EL} (O'Connor et al., 1998), and of these, at least two (Bim_L and Bim_{EL}) were clearly identifiable in Bcl-X_L immunoprecipitates. A further unidentified isoform was also noted migrating between Bim_L and Bim_{EL} (Figure 7B) that could represent a novel splice form (Marani et al., 2002). Overall, these results show that oncogenic $p56^{lck\text{-}F505}$ induces signaling pathway(s) that inhibit Bcl-X_L deamidation and that preserve its binding to the BH3-only protein Bim.

The workers who first described DNA-damage-induced Bcl-X_L deamidation showed that Retinoblastoma (Rb) expression caused inhibition of Bcl-X_L deamidation using their cell line system (Deverman et al., 2002). This is consistent with the demonstration that Rb is a potent inhibitor of apoptosis during the DNA damage response (Wang et al., 2001b). We therefore examined the expression and phosphorylation status of Rb in murine thymocytes. As expected, DNA damage triggered a characteristic shift in Rb migration due to its reduced phosphorylation and consequent activation. However, this was comparable in all four phenotypes, and we found no evidence that either Rb expression or Rb dephosphorylation was different in the $Lck^{F505}CD45^{-/-}$ compared to other thymocytes (Figure 7C).

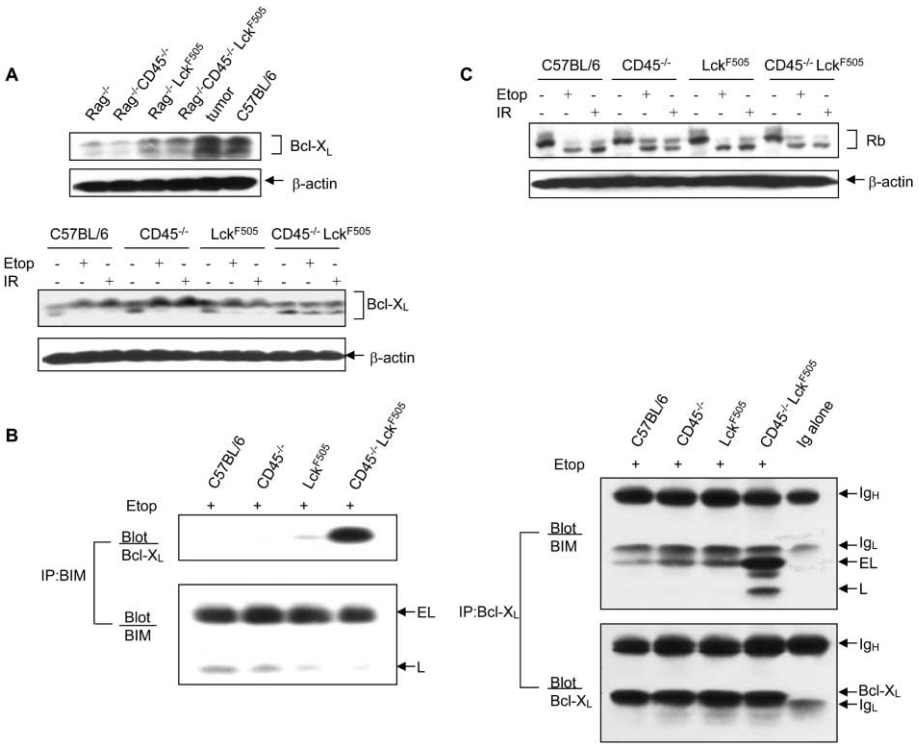

Figure 7. Oncogenic Lck^{F505} inhibits Bcl-X_L deamidation induced by DNA damage

A: Upper panel: DN thymocytes purified from Rag$^{-/-}$Lck^{F505} and Rag$^{-/-}$CD45$^{-/-}$Lck^{F505} mice (5 of each), or thymocytes from Rag$^{-/-}$, Rag$^{-/-}$CD45$^{-/-}$, and C57BL/6 mice, or Rag$^{-/-}$CD45$^{-/-}$Lck^{F505} tumor cells, were immunoblotted for Bcl-X_L. The membrane was stripped and reprobed for β actin to show comparable loading. Lower panel: DNA damage was induced as in Figure 5 and whole cell lysates then immunoblotted for Bcl-X_L.

B: Cells were treated with 20 μM etoposide for 24 hr and immunoprecipitations were performed using an antibody against Bim (left panel) or Bcl-X_L (right panel), respectively, followed by immunoblotting as indicated. Five separate experiments each were performed for the Bim and Bcl-X_L immunoprecipitations, respectively, with comparable results.

C: Immunoblotting of thymic lysates was carried out with a mAb recognizing both the phosphorylated and dephosphorylated forms of Rb.

Therefore, regulation of Rb expression or activation in response to DNA damage may not explain the inhibition of Bcl-X_L deamidation observed in thymocytes.

Discussion

The transgenic mouse lines investigated in this study provide an experimental system in which the distinctive transforming signals mediated by an oncogenic tyrosine kinase can be discriminated from the survival and proliferative signals that regulate early thymic differentiation. A 2- to 3-fold increase in p56^{lck} kinase activity (Figure 1) has the capacity, as Figure 8 illustrates, to switch on an ensemble of signals that are unique to the DN thymocytes destined to develop T cell lymphomas. This oncogenic ensemble includes the inhibition of DNA repair and the resulting increase in DNA damage (Figure 4), the inhibition of DNA-damage-induced Bcl-X_L deamidation (Figure 7A), the preservation of Bcl-X_L sequestering functionality (Figure 7B), and inhibition of Bax conformation change (Figure 6D), Bax mitochondrial translocation (Figure 6C), cytochrome c release (Figure 6C), and the apoptotic downstream caspase execution cascade (Figure 6). Out of this ensemble, the prevention of Bcl-X_L deamidation in the context of primary thymocytes undergoing transformation and the concomitant preservation of its ability to bind Bim are of particular interest. Our choice of Bim as an exemplar to test the ability of Bcl-X_L to sequester a BH3-only protein was based on our technical ability to measure endogenous Bcl-X_L-Bim interactions in primary murine thymocytes, thereby facilitating direct comparison with previous work performed using a transfected cell line (Deverman et al., 2002). Identification of the BH3-only protein(s) actually involved in the DNA damage response in DN thymocytes will require further analysis.

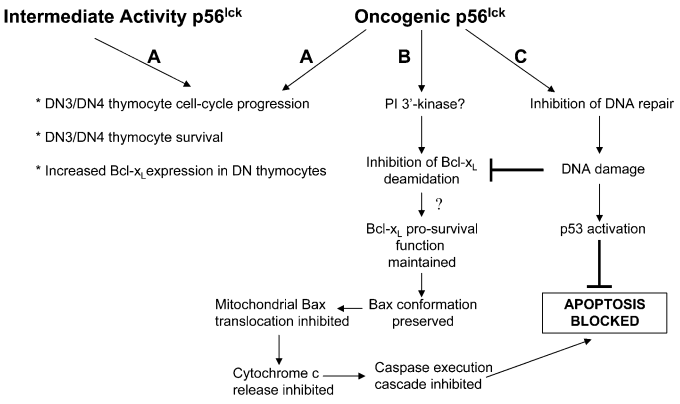

Figure 8. A model integrating the findings of this paper

Pathway A refers to signals that are common to both intermediate activity p56^{lck} (as in DN CD45$^{-/-}$ or Lck^{F505} thymocytes) and oncogenic p56^{lck} (as in DN CD45$^{-/-}$Lck^{F505} thymocytes). Pathways B and C are unique to the oncogenic hyperactive p56^{lck} found in DN CD45$^{-/-}$Lck^{F505} thymocytes.

Until recently, protein deamidation has been considered as a molecular timer, regulating protein turnover and function by the nonenzymatic deamidation of asparagine and glutamine residues (Robinson and Robinson, 2001). However, the finding that two critical internal Asn residues in Bcl-X_L, located within an unstructured loop separating the α1 (BH4 domain) and α2 (BH3 domain) helices, can be deamidated in vivo in response to DNA damage (Deverman et al., 2002) has suggested novel biological functions for protein deamidation. Our own findings suggest that inhibition of deamidation may be critical in the transforming events that lead to the development of T lymphomas. The tight correlation between inhibition of Bcl-X_L deamida-

tion and preservation of the Bcl-X_L-Bim interaction (Figure 7) suggests that these two events might be linked. However, a mutant version of Bcl-X_L in which Asn-52 and Asn-66 were changed to Asp residues has been reported to retain normal Bim binding (Deverman et al., 2003). On the other hand, deamidation of Asn residues typically leads to a preponderance of isoaspartate over aspartate residues (Aswad et al., 2000; Aritomi et al., 1997), so it remains possible that conversion of Asn-52 and Asn-66 to isoaspartates in vivo might prevent Bim binding. In addition, mutation of these Asn residues to Ala prevents Bcl-X_L deamidation and promotes the prosurvival functions of Bcl-X_L, indicating a possible link between deamidation and Bcl-X_L function (Deverman et al., 2002). Protein deamidation may also result in degradation (Sun et al., 1995), leading to increased Bcl-X_L turnover. Nevertheless, as Figure 7B illustrates, the preservation of Bcl-X_L-Bim binding in pretumorigenic thymocytes cannot be explained by inhibition of Bcl-X_L degradation. We therefore envisage that in wild-type thymocytes, BH3-only protein(s) are sequestered by preferential binding to Bcl-X_L (Letai et al., 2002), so preventing their binding to Bax, in turn maintaining Bax in a conformational state that disfavors its translocation and oligomerization in mitochondrial membranes (Figure 7) (Cheng et al., 2001; Marani et al., 2002). Following DNA damage, Bcl-X_L is deamidated and its ability to sequester BH3-only proteins is compromised, causing their release and interaction with Bax, consequently triggering Bax mitochondrial translocation and the subsequent release of cytochrome c and activation of the execution caspases (Figure 6). By inhibiting the DNA-damage-triggered changes in Bcl-X_L, hyperactive $p56^{lck\text{-}F505}$ thereby disrupts the cancer protection pathway that normally disposes of cells with damaged DNA. Increased Bcl-X_L expression in response to an OTK (Figure 7A), as described for OTKs such as BCR-ABL (Amarante-Mendes et al., 1998), may therefore prove to be necessary but not sufficient for transformation. Of course we also cannot exclude the possibility that other $p56^{lck\text{-}F505}$-driven survival pathways contribute to oncogenesis.

It is intriguing that whereas "intermediate activity" $p56^{lck\text{-}F505}$ was almost 100% efficient at rescuing $Rag^{-/-}$ DN3 cells from apoptosis due to the failure of β selection (Figure 2), this kinase activity level was incapable of rescuing the same cells from DNA-damage-induced apoptosis (Figure 5A). Presumably, intermediate activity $p56^{lck\text{-}F505}$ mimics pre-TCR mediated survival signals such as p53 inactivation and NFκB activation in order to rescue DN3 thymocytes from apoptosis so completely (Haks et al., 1999), although we have not specifically investigated these pathways. We assume that it is the additional level of regulation of Bcl-2 family members such as Bcl-X_L in the context of DNA damage that renders the hyperactive version of $p56^{lck\text{-}F505}$ oncogenic. Importantly, Bcl-X_L expression per se does not appear essential for the progression of DN3 thymocytes through the β selection checkpoint, consistent with this interpretation (Ma et al., 1995).

The lethal combination of reduced DNA repair (Figure 4A) in conjunction with protection from DNA-damage-induced apoptosis (Figure 5A) is a potent predicator of genomic instability (Figures 4B and 4C). Genomic instability is increased as a consequence of V(D)J recombination events in DN2/DN3 thymic subsets (Bassing et al., 2002). In light of the inhibition of DSB repair noted in $Lck^{F505}CD45^{-/-}$ thymocytes (Figure 4A), it might therefore seem surprising that the survival curves of $Lck^{F505}CD45^{-/-}$ mice are not affected by a Rag-$1^{-/-}$ background (Baker et al., 2000). However, mutant Lck^{F505} inhibits V(D)J recombination, causing premature allelic exclusion (Anderson et al., 1993), so in any case, the level of DSBs produced by the Rag enzymes is likely to be less in this context. Of possibly greater significance is the DN3/DN4 proliferation induced by the active Lck^{F505} transgene (Figure 3A): it is presumably the reduction in DSB repair during subsequent cell divisions that leads to the accumulation of DNA damage in pretumorigenic $Lck^{F505}CD45^{-/-}$ cells, consistent with the increase in basal γH2AX (Figure 4A) and p53 activation (Figure 5D). Even small numbers of DSBs can be lethal, particularly if they occur during the replication of the genome and, if not repaired correctly, lead to chromosomal abnormalities (Khanna and Jackson, 2001).

An important conclusion from the present work is that a modest 2- to 3-fold increase in activity of an OTK, brought about in this case by CD45-deficiency (Figure 1), can convert the kinase into an oncogene. Indeed, the key differences between Lck^{F505} and $Lck^{F505}CD45^{-/-}$ thymocytes in response to DNA damage (Figure 8) are all-or-nothing: the mutant Lck^{F505} transgene in a $CD45^{+/+}$ environment neither inhibits DNA repair (Figure 4A) nor provides protection from DNA-damage-induced apoptosis (Figures 5–7). The 2- to 3-fold increase in $p56^{lck\text{-}F505}$ activity therefore appears to control a molecular switch rather than a rheostat mechanism.

Although the present study was carried out on pretumorigenic cells that displayed no overt signs of neoplasia, we have shown that hyperactive Lck^{F505} causes high Bcl-X_L expression in $Lck^{F505}CD45^{-/-}$ lymphoma cells (Figure 7A), and preliminary results (not shown) indicate that in this context Bcl-X_L deamidation is also inhibited following DNA damage. A survey of the 60 cell lines in an anticancer drug screen panel has previously shown a striking correlation between Bcl-X_L expression and resistance to a wide range of genotoxic compounds (Amundson et al., 2000). Furthermore, OTKs such as BCR-ABL are known to upregulate Bcl-X_L (Amarante-Mendes et al., 1998), and the resistance of OTK-expressing tumors to chemo- and radiotherapy represents one of the main causes of failure of antitumor treatments (Skorski, 2002). It therefore seems feasible that pharmaceutical intervention to counteract the inhibition of the DNA-damage-induced Bcl-X_L modifications described in the present work would not only prevent tumorigenesis caused by the actions of an OTK, but could also promote the apoptosis of tumor cells in response to genotoxic agents.

Experimental procedures

Mice

All mice were bred and housed in specific pathogen-free conditions in the animal facility at The Babraham Institute, Cambridge, UK. The $p56^{Lck\text{-}F505}$ (PLGF-A) transgenic mice (Abraham et al., 1991) and the $CD45^{-/-}$, $CD45^{-/-}Lck^{F505}$, $Rag^{-/-}$ Lck^{F505}, and $Rag^{-/-}CD45^{-/-}Lck^{F505}$ mice have been previously described (Baker et al., 2000).

Flow cytometry

Three-color or four-color analyses were carried out using a FACSCalibur (Becton Dickinson). The following mAbs, labeled with FITC, PE, PerCP, or Biotin, were purchased from Pharmingen (San Diego): CD4 (L3T4), CD8 (53-6.7), CD3ε (500A2), CD44 (Ly24), CD25 (PC61), NK1.1 (PK136), CD11B (M1/70), CD11C (HL3), B220 (RA3-6B2), Bcl-2 (3F11), γH2AX, and respective isotype controls. Streptavidin-APC (Caltag, Burlingame) was used to detect biotinylated mAbs. TUNEL (Tdt-mediated dUTP nick end labeling) staining of apoptotic cells employed the In Situ Cell Death Detection kit from Roche (Mannheim, Germany). DNA staining was with 7-amino-actinomycin D

(7-AAD). DN3 and DN4 subsets were analyzed by first gating out thymocytes staining positive for biotinylated mAbs to CD3e, CD4, CD8, CD44, NK1.1, CD11B, CD11C, and B220, followed by Streptavidin-FITC or Streptavidin-APC. PE or PerCP-conjugated CD25 mAb was then used to identify the DN3 subset, the $CD25^-$ cells representing the DN4 subset.

BrdU labeling

Mice were injected i.p. with 1 mg BrdU, and thymi were removed after 2 hr. Cells were first stained for surface antigen, and then fixed in 95% ethanol. After 30 min on ice, cells were washed and resuspended in PBS with 1% paraformaldehyde and 0.05% Tween 20, with incubation for 30 min at room temperature. The cells were then centrifuged and resuspended in PBS supplemented with 4.2 mM $Mgcl_2$, 10 μM HCL, and 100 U of DNase I. After incubation at 25°C for 30 min, the cells were washed and stained with BrdU-FITC antibody (Becton Dickinson) for FACS analysis.

Purification of DN thymocytes

Total thymocytes were incubated with CD3, CD4, and CD8 biotin-conjugated antibodies, washed, and mixed with Dynabeads M-280 Streptavidin (Dynal, Oslo, Norway) with gentle rotation at 4°C for 30 min. The immobilized cells were isolated using a Magnetic Particle Concentrator (Dynal MPC). The procedure was repeated once more to generate >97% pure DN thymocytes (see Supplemental Figure S1 at http://www.cancercell.org/cgi/content/full/5/1/37/DC1).

DNA damage treatments

Freshly isolated thymocytes were irradiated by 10 Gy using a cesium source unless otherwise indicated, then incubated for 24 hr; or treated with etoposide for 24 hr at a concentration of 50 μM unless otherwise indicated.

Subcellular fractionation

Cells were washed in ice-cold PBS and resuspended in five vols of isotonic mitochondria buffer: 210 mM mannitol, 70 mM sucrose, 1 mM EDTA, 1 mM EGTA, 10 mM Hepes (pH 7.5), and Complete Protease Inhibitors (Roche). After 30 min incubation on ice, cells were homogenized and centrifuged at 1000 × g for 10 min at 4°C. The supernatants were then centrifuged at 13,000 × g for 15 min at 4°C to obtain the pelleted mitochondrial fraction. The supernatants were further centrifuged at 100,000 × g for 90 min at 4°C, and the resulting supernatants designated as the cytosolic (S-100) fraction.

Immunoblotting

The following antibodies were used: p53 (pab240), Mdm2 (smp-14), $p21^{WAF1}$ (c-9), PARP (H-20), and H2A (H-124) from Santa Cruz; phospho-p53 (pSer15), caspase-3, phospho-Lck (Tyr 505), and γH2AX from Cell Signaling (Beverly); phospho-Lck (Tyr 394) was from A. Shaw (Washington University School of Medicine; see Holdorf et al., 2002); Bax was from Upstate (New York); cytochrome c, 6A7, Rb, Bim from Pharmingen (San Diego); Bcl-x, Lck from Transduction Lab (New Jersey); COX-IV from Molecular Probes (Eugene); β actin from Sigma (Steinheim, Germany).

Immunoprecipitation

Cells were lysed in 50 mM HEPES (pH 7.2), 150 mM NaCl, 1 mM EDTA, 0.2% NP-40, and Complete Protease Inhibitors. For immunoprecipitation of Bim, rat Bim ab (Oncogene, San Diego) was coated to goat-anti-rat Ig-Agarose (Sigma); for immunoprecipitation of Bcl-xl, rabbit-anti-Bcl-xl ab (Cell Signaling) was coated to goat-anti-rabbit Ig-Agarose (Sigma). Lysates were precleared with appropriate Agarose. For immunoprecipitation of Lck, rabbit anti-Lck ab (Pharmingen) was coated to Protein G-Sepharose (Amersham, Uppsala, Sweden) and lysates were precleared with Protein G-Sepharose. Quantification of immunoblots was carried out using a phosphorimager (Fuji FLA3000).

Pulse-field gel electrophoresis

Purified DN thymocytes were irradiated at a dose of 80 Gy; samples were taken immediately, 6 hr or 24 hr after incubation at 37°C. Samples were resuspended at 5×10^7 cells/ml in 0.6% low-melting-point agarose (Bio-Rad) cast into an agarose plug (75 μl). Lysates were obtained by treatment with Proteinase K. Clamped homogenous electric field (CHEF) gel electrophoresis (CHEF-DRII, Bio-Rad) was used to separate DNA containing DSBs from intact DNA (3 v/cm, pulsed from 600–900 s for 24 hr, then 900 s for 24 hr). Chromosomal DNA size markers *S. pombe* and *H. wingei* were from Biorad. Gels were stained with ethidium bromide and quantification of DNA was obtained by phosphorimager analysis. The percentage of DNA containing DSBs was determined as the integral density value of released DNA from the plug/total DNA.

Karyotype analysis by chromosome painting

Purified DN thymocytes were cultured in RPMI media supplemented with 10% FCS, L-Glutamine 1 mM, Pen/Strep 200 μg/ml, IL-4 10 ng/ml, and PdBu 30 ng/ml. Cells were harvested 44 hr later. Mouse metaphases were prepared according to standard procedures. Mouse chromosome-specific probes were made by degenerate oligonucleotide primed PCR from flow-sorted chromosomes according to the methods previously described (Ferguson-Smith, 1997; Telenius et al., 1992). Mouse rainbow FISH probe (Cambio, Cambridge), which contains three sets of 7-color labeled mouse chromosome-specific paints (i.e., P1: chrs. 1–7; P2: chrs. 8–14; and P3: chrs. 15–Y), were used in this study following the manufacturer's protocols. Each set of probes allows the simultaneous visualization of seven mouse chromosomes in one hybridization and thus the entire mouse genome in three hybridizations. Chromosome painting and digital image analysis followed the methods described in Yang et al. (1995).

Acknowledgments

We are grateful to Dr. Julia Marley for analyzing Bcl-2 expression, to Cindy Webb for her assistance with animal husbandry, to Geoff Morgan for assistance with FACS, to Prof. Ashok Venkitaraman and Beatriz Goyenechea for advice on DNA damage techniques, to Prof. Andrey Shaw for supply of a reagent, and to the Biotechnology and Biological Sciences Research Council for financial support.

Received: May 2, 2003
Revised: November 5, 2003
Accepted: November 24, 2003
Published: January 19, 2004

References

Abraham, K.M., Levin, S.D., Marth, J.D., Forbush, K.A., and Perlmutter, R.M. (1991). Thymic tumorigenesis induced by overexpression of P56lck. Proc. Natl. Acad. Sci. USA *88*, 3977–3981.

Alexander, D.R. (1997). The role of the CD45 phosphotyrosine phosphatase in lymphocyte signalling. In Lymphocyte Signalling: Mechanisms, Subversion and Manipulation, M.M. Harnett and K.P. Rigley, eds. (Sussex, England: John Wiley & Sons Ltd.), pp. 107–140.

Alexander, D.R. (2000). The CD45 tyrosine phosphatase: a positive and negative regulator of immune cell function. Semin. Immunol. *12*, 349–359.

Amarante-Mendes, G.P., McGahon, A.J., Nishioka, W.K., Afar, D.E., Witte, O.N., and Green, D.R. (1998). Bcl-2-independent BCR-ABL-mediated resistance to apoptosis: protection is correlated with up regulation of Bcl-xL. Oncogene *16*, 1383–1390.

Amundson, S.A., Myers, T.G., Scudiero, D., Kitada, S., Reed, J.C., and Fornace, A.J. (2000). An informatics approach identifying markers of chemosensitivity in human cancer cell lines. Cancer Res. *60*, 6101–6110.

Anderson, S.J., Levin, S.D., and Perlmutter, R.M. (1993). Protein-tyrosine kinase p56(Lck) controls allelic exclusion of T-cell receptor beta-chain genes. Nature *365*, 552–554.

Aritomi, M., Kunishima, N., Inohara, N., Ishibashi, Y., Ohta, S., and Morikawa, K. (1997). Crystal structure of rat bcl-x_L. J. Biol. Chem. *272*, 27886–27892.

Aswad, D.W., Paranandi, M.V., and Schurter, B.T. (2000). Isoaspartate in peptides and proteins: formation, significance, and analysis. J. Pharm. Biomed. Anal. *21*, 1129–1136.

Baker, M., Gamble, J., Tooze, R., Higgins, D., Yang, F.T., O'Brien, P.C.M., Coleman, N., Pingel, S., Turner, M., and Alexander, D.R. (2000). Development

of T-leukaemias in CD45 tyrosine phosphatase-deficient mutant lck mice. EMBO J. *19*, 4644–4654.

Bassing, C.H., Swat, W., and Alt, F.W. (2002). The mechanism and regulation of chromosomal V(D)J recombination. Cell *109* (*Suppl*), S45–S55.

Bassing, C.H., Suh, H., Ferguson, D.O., Chua, K.F., Manis, J., Eckersdorff, M., Gleason, M., Bronson, R., Lee, C., and Alt, F.W. (2003). Histone H2AX: A dosage-dependent suppressor of oncogenic translocations and tumors. Cell *114*, 359–370.

Bullock, A.N., and Fersht, A.R. (2001). Rescuing the function of mutant p53. Nat. Rev. Cancer *1*, 68–76.

Byth, K.F., Conroy, L.A., Howlett, S., Smith, A.J.H., May, J., Alexander, D.R., and Holmes, N. (1996). CD45-null transgenic mice reveal a positive regulatory role for CD45 in early thymocyte development, in the selection of CD4(+)CD8(+) thymocytes, and in B-cell maturation. J. Exp. Med. *183*, 1707–1718.

Cheng, E.H., Wei, M.C., Weiler, S., Flavell, R.A., Mak, T.W., Lindsten, T., and Korsmeyer, S.J. (2001). BCL-2, BCL-X(L) sequester BH3 domain-only molecules preventing BAX- and BAK-mediated mitochondrial apoptosis. Mol. Cell *8*, 705–711.

Cohen, G.M., Sun, X.M., Fearnhead, H., MacFarlane, M., Brown, D.G., Snowden, R.T., and Dinsdale, D. (1994). Formation of large molecular weight fragments of DNA is a key committed step of apoptosis in thymocytes. J. Immunol. *153*, 507–516.

De Silva, I.U., McHugh, P.J., Clingen, P.H., and Hartley, J.A. (2000). Defining the roles of nucleotide excision repair and recombination in the repair of DNA interstrand cross-links in mammalian cells. Mol. Cell. Biol. *20*, 7980–7990.

Deutsch, E., Dugray, A., AbdulKarim, B., Marangoni, E., Maggiorella, L., Vaganay, S., M'Kacher, R., Rasy, S.D., Eschwege, F., Vainchenker, W., et al. (2001). BCR-ABL down-regulates the DNA repair protein DNA-PKcs. Blood *97*, 2084–2090.

Deverman, B.E., Cook, B.L., Manson, S.R., Niederhoff, R.A., Langer, E.M., Rosova, I., Kulans, L.A., Fu, X., Weinberg, J.S., Heinecke, J.W., et al. (2002). Bcl-xL deamidation is a critical switch in the regulation of the response to DNA damage. Cell *111*, 51–62.

Deverman, B.E., Cook, B.L., Manson, S.R., Niederhoff, R.A., Langer, E.M., Rosová, I., Kulans, L.A., Fu, X., Weinberg, J.S., Heinecke, J.W., et al. (2003). Erratum to: Bcl-x_L deamidation is a critical switch in the regulation of the response to DNA damage. Cell *115*, 503.

Falk, I., Nerz, G., Haidl, I., Krotkova, A., and Eichmann, K. (2001). Immature thymocytes that fail to express TCRbeta and/or TCRgamma delta proteins die by apoptotic cell death in the CD44(-)CD25(-) (DN4) subset. Eur. J. Immunol. *31*, 3308–3317.

Ferguson-Smith, M.A. (1997). Genetic analysis by chromosome sorting and painting: phylogenetic and diagnostic applications. Eur. J. Hum. Genet. *5*, 253–265.

Gross, A., Jockel, J., Wei, M.C., and Korsmeyer, S.J. (1998). Enforced dimerization of BAX results in its translocation, mitochondrial dysfunction and apoptosis. EMBO J. *17*, 3878–3885.

Haks, M.C., Krimpenfort, P., van den Brakel, J.H.N., and Kruisbeek, A.M. (1999). Pre-TCR signalling and inactivation of p53 induces crucial cell survival pathways in pre-T cells. Immunity *11*, 91–101.

Hanahan, D., and Weinberg, R.A. (2000). The hallmarks of cancer. Cell *100*, 57–70.

Hengartner, M.O. (2000). The biochemistry of apoptosis. Nature *407*, 770–776.

Holdorf, A.D., Lee, K.H., Burack, W.R., Allen, P.M., and Shaw, A.S. (2002). Regulation of Lck activity by CD4 and CD28 in the immunological synapse. Nat. Immunol. *3*, 259–264.

Hsu, Y.T., and Youle, R.J. (1998). Bax in murine thymus is a soluble monomeric protein that displays differential detergent-induced conformations. J. Biol. Chem. *273*, 10777–10783.

Huang, D.C., and Strasser, A. (2000). BH3-Only proteins-essential initiators of apoptotic cell death. Cell *103*, 839–842.

Jain, S.K., Susa, M., Keeler, M.L., Carlesso, N., Druker, B., and Varticovski, L. (1996). PI 3-kinase activation in BCR/abl-transformed hematopoietic cells does not require interaction of p85 SH2 domains with p210 BCR/abl. Blood *88*, 1542–1550.

Khanna, K.K., and Jackson, S.P. (2001). DNA double-strand breaks: signaling, repair and the cancer connection. Nat. Genet. *27*, 247–254.

Kumar, R., Mandal, M., Lipton, A., Harvey, H., and Thompson, C.B. (1996). Overexpression of Her2 modulates Bcl-2, Bcl-X(L), and tamoxifen-induced apoptosis in human Mcf-7 breast-cancer cells. Clin. Cancer Res. *2*, 1215–1219.

Kuwana, T., Mackey, M.R., Perkins, G., Ellisman, M.H., Latterich, M., Schneiter, R., Green, D.R., and Newmeyer, D.D. (2002). Bid, Bax, and lipids cooperate to form supramolecular openings in the outer mitochondrial membrane. Cell *111*, 331–342.

Letai, A., Bassik, M.C., Walensky, L.D., Sorcinelli, M.D., Weiler, S., and Korsmeyer, S.J. (2002). Distinct BH3 domains either sensitize or activate mitochondrial apoptosis, serving as prototype cancer therapeutics. Cancer Cell *2*, 183–192.

Lin, K., Longo, N.S., Wang, X., Hewitt, J.A., and Abraham, K.M. (2000). Lck domains differentially contribute to pre-T cell receptor (TCR)- and TCR-alpha/beta-regulated developmental transitions. J. Exp. Med. *191*, 703–716.

Ma, A., Pena, J.C., Chang, B., Margosian, E., Davidson, L., Alt, F.W., and Thompson, C.B. (1995). Bclx regulates the survival of double-positive thymocytes. Proc. Natl. Acad. Sci. USA *92*, 4763–4767.

Marani, M., Tenev, T., Hancock, D., Downward, J., and Lemoine, N.R. (2002). Identification of novel isoforms of the BH3 domain protein Bim which directly activate Bax to trigger apoptosis. Mol. Cell. Biol. *22*, 3577–3589.

Nechushtan, A., Smith, C.L., Hsu, Y.T., and Youle, R.J. (1999). Conformation of the Bax C-terminus regulates subcellular location and cell death. EMBO J. *18*, 2330–2341.

O'Connor, L., Strasser, A., O'Reilly, L.A., Hausmann, G., Adams, J.M., Cory, S., and Huang, D.C. (1998). Bim: a novel member of the Bcl-2 family that promotes apoptosis. EMBO J. *17*, 384–395.

Pingel, S., Baker, M., Turner, M., Holmes, N., and Alexander, D.R. (1999). The CD45 tyrosine phosphatase regulates CD3-induced signal transduction and T cell development in recombinase-deficient mice: restoration of pre-TCR function by active p56(lck). Eur. J. Immunol. *29*, 2376–2384.

Richardson, C., and Jasin, M. (2000). Frequent chromosomal translocations induced by DNA double-strand breaks. Nature *405*, 697–700.

Robinson, N.E., and Robinson, A.B. (2001). Molecular clocks. Proc. Natl. Acad. Sci. USA *98*, 944–949.

Rodewald, H.R., and Fehling, H.J. (1998). Molecular and cellular events in early thymocyte development. Adv. Immunol. *69*, 1–112.

Rodriguez, J., and Lazebnik, Y. (1999). Caspase-9 and APAF-1 form an active holoenzyme. Genes Dev. *13*, 3179–3184.

Rogakou, E.P., Pilch, D.R., Orr, A.H., Ivanova, V.S., and Bonner, W.M. (1998). DNA double-stranded breaks induce H2AX phosphorylation on serine 139. J. Biol. Chem. *273*, 5858–5868.

Salomoni, P., Condorelli, F., Sweeney, S.M., and Calabretta, B. (2000). Versatility of BCR/ABL-expressing leukemic cells in circumventing proapoptotic BAD effects. Blood *96*, 676–684.

Sherr, C.J., and McCormick, F. (2002). The RB and p53 pathways in cancer. Cancer Cell *2*, 103–112.

Siliciano, J.D., Canman, C.E., Taya, Y., Sakaguchi, K., Appella, E., and Kastan, M.B. (1997). DNA damage induces phosphorylation of the amino terminus of p53. Genes Dev. *11*, 3471–3481.

Simbulan-Rosenthal, C.M., Rosenthal, D.S., Iyer, S., Boulares, H., and Smulson, M.E. (1999). Involvement of PARP and poly(ADP-ribosyl)ation in the early stages of apoptosis and DNA replication. Mol. Cell. Biochem. *193*, 137–148.

Skorski, T. (2002). Oncogenic tyrosine kinases and the DNA-damage response. Nat. Rev. Cancer *2*, 351–360.

Slupianek, A., Hoser, G., Majsterek, I., Bronisz, A., Malecki, M., Blasiak, J., Fishel, R., and Skorski, T. (2002). Fusion tyrosine kinases induce drug resistance by stimulation of homology-dependent recombination repair, prolongation of G(2)/M phase, and protection from apoptosis. Mol. Cell. Biol. *22*, 4189–4201.

Stone, J.D., Conroy, L.A., Byth, K.F., Hederer, R.A., Howlett, S., Takemoto, Y., Holmes, N., and Alexander, D.R. (1997). Aberrant TCR-mediated signalling in CD45-null thymocytes involves dysfunctional regulation of Lck, Fyn, TCR-ζ and ZAP-70. J. Immunol. *158*, 5773–5782.

Sun, A.Q., Yuksel, K.U., and Gracy, R.W. (1995). Terminal marking of triosephosphate isomerase: consequences of deamidation. Arch. Biochem. Biophys. *322*, 361–368.

Telenius, H., Pelmear, A.H., Tunnacliffe, A., Carter, N.P., Behmel, A., Ferguson-Smith, M.A., Nordenskjold, M., Pfrangner, R., and Ponder, B.A. (1992). Cytogenetic analysis by chromosome painting using DOP-PCR amplified flow-sorted chromosomes. Genes Chromosomes Cancer *4*, 256–263.

Vousden, K.H., and Lu, X. (2002). Live or let die: the cell's response to p53. Nat. Rev. Cancer *2*, 594–604.

Wang, Z.H., Ding, M.X., Yuan, J.P., Jin, M.L., Hao, C.F., Chew-Cheng, S.B., Ng, H.K., and Chew, E.C. (1999). Expression of bcl-2 and Bax in EGFR-antisense transfected and untransfected glioblastoma cells. Anticancer Res. *19*, 4167–4170.

Wang, X. (2001a). The expanding role of mitochondria in apoptosis. Genes Dev. *15*, 2922–2933.

Wang, J.Y., Naderi, S., and Chen, T.T. (2001b). Role of retinoblastoma tumor suppressor protein in DNA damage response. Acta Oncol. *40*, 689–695.

Yang, F., Carter, N.P., Shi, L., and Ferguson-Smith, M.A. (1995). A comparative study of karyotypes of muntjacs by chromosome painting. Chromosoma *103*, 642–652.

Zlotnik, A., Ransom, J., Frank, G., Fischer, M., and Howard, M. (1987). Interleukin 4 is a growth factor for activated thymocytes: possible role in T-cell ontogeny. Proc. Natl. Acad. Sci. USA *84*, 3856–3860.

Zou, H., Li, Y., Liu, X., and Wang, X. (1999). An APAF-1.cytochrome c multimeric complex is a functional apoptosome that activates procaspase-9. J. Biol. Chem. *274*, 11549–11556.